Lab on a Chip

ARTICLE

Fabrication of monodisperse alginate microgel beads by microfluidic picoinjection: A chelate free approach

Received 00th January 20xx,
Accepted 00th January 20xx

DOI: 10.1039/x0xx00000x

www.rsc.org/

Husnain Ahmed and Bjørn Torger Stokke*

Micron-sized alginate hydrogel beads are extensively employed as an encapsulation medium for biochemical and biomedical applications. Here we report on the microfluidic assisted fabrication of calcium alginate (Ca-alginate) beads by on-chip picoinjection of aqueous calcium chloride ($CaCl_2$) in emulsified aqueous sodium alginate (Na-alginate) droplets or by picoinjection of Na-alginate solution in emulsified aqueous $CaCl_2$ droplets. There is no added chelator to reduce the Ca activity in either of the two strategies. The two fabrication strategies are implemented using a flow-focusing and picoinjection modules in a single PDMS chip. Aqueous alginate solution was emulsified and infused with $CaCl_2$ solution as the squeezed droplet pass the picoinjection channel; consequently, monodisperse, spherical, and structurally homogeneous Ca-alginate beads were obtained. Monodisperse alginate microgel populations with a mean diameter in the range of 8 to 28 µm and standard deviation less than 1 µm were successfully generated using microfluidic channels with various dimensions and controlling the flow parameters. Monodisperse but also non-spherical particles with diameters 6 to 15 µm were also fabricated when picoinjecting Na-alginate solution in emulsified aqueous $CaCl_2$ droplets. The Ca-alginate microbeads fabricated with tailormade size in the range from sub-cellular and upwards were in both strategies realized without any use of chelators or change in pH conditions, which is considered a significant advantage for further exploitation as encapsulation process for improved enzymatic activity and cell viability.

Introduction

Hydrogels are being preferred for numerous applications in pharmaceutical research, drug delivery, tissue engineering, and food science.[1–4] Alginate, a natural polysaccharide found in brown seaweed, is widely explored in the biomedical field due to the combination of mild gelation conditions and its biocompatible, biodegradable and non-toxic nature.[1,5,6] Micron-sized alginate gel beads that mimic properties of the extracellular matrices in tissues are widely used to encapsulate, cultivate, and monitor living cells.[7–14] Typically, alginate gel beads are prepared in the process of ionic crosslinking when an aqueous alginate solution interacts with divalent cations such as Ca^{2+} in an encapsulation process.

The ionotropic alginate gelation is exploited based on, for example, dripping sodium alginate aqueous solution into the excess of aqueous solutions of crosslinking ions as a straightforward approach to generate gel beads in the size-range 200 µm to several mm.[15–18] Moreover, electrostatic extrusion,[19,20] airflow nozzles,[21], and micro-nozzle array[22] are explored. However, these strategies have limitations in producing monodisperse and small-sized particles (<100 µm). The translation of the process to microdevices to support the generation of monodisperse, structurally homogeneous, and smaller gel beads has proven challenging. The challenge is associated with the rapid transformation from the solution to the gel state of alginate solution on exposure to gel-inducing ions. This particularity makes it difficult to perform the gelation process into a microfluidic device to control the beads' size with dimensions less than 200 µm. Coflowing two solutions, one of aqueous alginate without the gelling ion and the other with the gelling ion (Ca^{2+}), result in clogging of the miniaturized channels in the region where the two streams meet due to the rapid ionic crosslinking.[23]

Current microfluidic assisted fabrication strategies for the preparation of ionotropic gel beads with sizes less than 200 µm are based on reducing the activity of the gelation ion in the (flow-focusing) emulsification step followed by post-emulsification ionotropic gelation.

For instance, Zhang *et al.*[24] proposed an idea to generate alginate drops containing water-insoluble salts of divalent ions (e.g., $CaCO_3$ nanoparticles) in a microfluidic device, followed by exposing the generated emulsions droplets to acidic conditions resulting in the dissolution of Ca and making them available for interaction with alginate. This method separated the drop formation step, and gelation reaction and monodisperse gel particles were obtained. However, alongside the pH reduction, the heterogeneous distribution of Ca^{2+} ions due to the initial particulate nature of the Ca-source inside the pre-gel alginate drops resulted in poor homogeneity of the resulting alginate beads.

Biophysics and Medical Technology, Dept. of Physics, NTNU, Norwegian University of Science and Technology, NO-7491 Trondheim, Norway.
E-mail: bjorn.stokke@ntnu.no
Electronic Supplementary Information (ESI) available: Additional schematic, results, and experimental details. See DOI: 10.1039/x0xx00000x

The problem associated with poor homogeneity in the gel bead has been addressed by swapping the Ca source from $CaCO_3$ nanoparticles to using chelator to reduce the Ca activity of the ions and at the same time allow dispersion of the ionotropic ion in the pre-gel state, including the emulsification step, followed by the addition of H^+ source in the continuous phase (e.g., acetic acid in the fluorinated oil).[25] Diffusion of H^+ into the aqueous emulsified droplet reduces the pH, with the concomitant reduction of the association constant of the chelate – ion pair, thus making this ion accessible for the gelation of the polymer (alginate).[26] Although this approach yields structurally homogenous ionically crosslinked alginate gel beads, the low pH needed for the process yields conditions that significantly reduced the lifespan of immobilized, pH-sensitive cells. One example of the latter is the reported 60% viability after 15 min of mesenchymal stem cells immobilized in alginate microbeads prepared in a microfluidic device using Ca-EDTA as the Ca source, exposing the beads to acetic acid following the emulsification. [25] Further increase of the time of immobilized stem cells under those conditions were, however, found to reduce the viable fraction further, and no cells were viable after 30 min.

The challenge associated with the reduced pH can be relaxed using the process of competitive ligand exchange reaction proceeding at constant pH that can be selected by choice of chelators and process parameters, also at a pH compatible with living cell requirements (e.g., to be chosen by the user in the range 8 to 5, at least).[27] In this strategy, two aqueous alginate solutions, one with added gelling ion chelated with a gelling-ion chelator, and one solution of alginate with an exchange ion complexed with another chelator, are introduced into a dual inlet device where the two solutions are combined just before the flow-focusing emulsification. The gelling ion-chelator combination and exchange ion-chelator combination need to be selected to fulfill the order of association constants for a cascading exchange when combining these two solutions and releasing the gel-inducing ions to be accessible to interact with the polymer (alginate). Thus, the process allows the generation of homogenous and ionically crosslinked alginate hydrogels compatible with living cell conditions and combined with controlling the size of the gel bead cohorts in less than 200 µm, typically in the range below 50 µm in diameter. This strategy has furthermore been employed for encapsulation of Bacillus subtilis for enhancement of lipase production.[28] Nevertheless, the presence of the chelator (EDTA, ethylenediaminetetraacetic acid) complexed with the exchange ion in the alginate beads could decrease cellular performance because the chelator attracts metal ions such as Fe, Cu, Zn, Co that work as a cofactor for enzymatic activity.[29]

In the present work, we address the issue of the need to use crosslinking ions with reduced activity in the emulsification/process that, in some cases, can limit applicability. Also, chelated-ion complexes are avoided due to

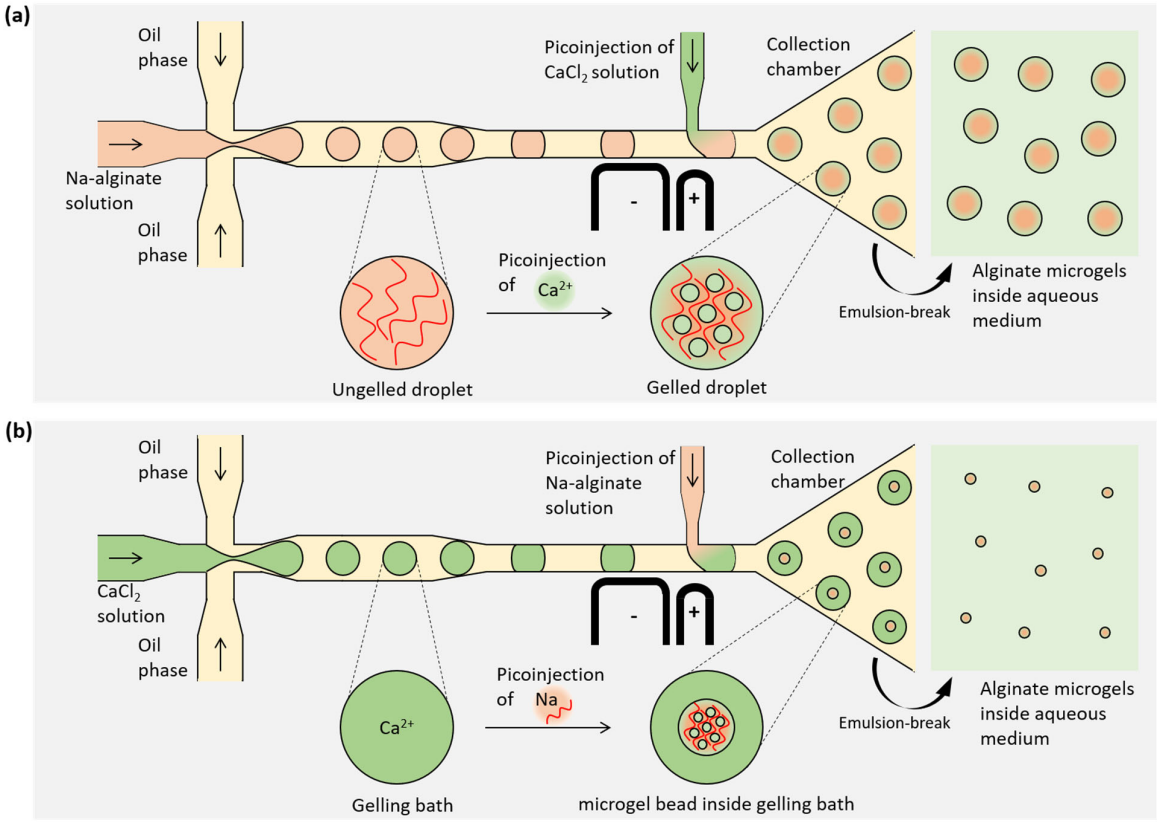

Fig. 1 Schematic diagrams of the device-assisted chelate free fabrication of homogenous sized populations of ionic crosslinked alginate microgel beads by (a) the picoinjection of chelate free aqueous $CaCl_2$ in emulsion droplets of aqueous Na-alginate and by (b) the picoinjection of Na-alginate solution in $CaCl_2$ emulsified droplets.

possible adverse effects, e.g., on activities of immobilized enzymes if remaining in the final bead. The approach presented here includes the combination of a device and a process for chelate free ionic crosslinking to fabricate monodisperse, homogeneous populations of alginate beads with a size typically less than 30 µm. A core element in the proposed process is the picoinjection of one aqueous solution into another emulsified droplet, where the two solutions either contain the alginate solution or the gelling ions solution. A core feature of the approach is that the micron-sized picoinjector limits the solution's contact area to be picoinjected, and the emulsified droplet, therefore, significantly reduced the chances of channel clogging due to the fast-ionic crosslinking. The proposed method contrasts with the coflowing technique used in microgel bead synthesis with more extended contact areas and thus requires other means to reduce possible clogging of the channels.

We report monodisperse production, structurally homogenous alginate particles in size range of 8-28 µm by the picoinjection of chelate free aqueous $CaCl_2$ in an aqueous sodium alginate drop. In the reverse strategy, the picoinjection of aqueous sodium alginate to emulsified chelate free aqueous $CaCl_2$ drops resulted in alginate microgels in a size range of 5-20 µm. Due to no change in the pH condition, the synthesized alginate microbeads are likely to be less invasive in the long-term cell culturing for different behavioral studies.

Experimental Section

Device fabrication

The PDMS microfluidic devices were fabricated by using a widespread used soft lithography process. A negative photoresist (mr DWL-40) was uniformly spin-coated on a 4" precleaned silicon wafer followed by substrate exposure to UV light through MLA-150 (maskless aligner) to transfer the custom-designed microfluidic channel design (Fig. S1) programmed in Clewin 4 (a layout editor) onto the substrate. The exposed pattern was developed, and the resulting master mold was surface treated by exposure to trichloro (1H, 1H, 2H, 2H-perfluorooctyl) silane (Sigma-Aldrich) under vacuum before the soft lithography.[30] A degassed mixture of PDMS base and curing agent (Sylgard 184A & 185B, Dow corning) in a 10:1 ratio was poured on top of the master mold and cured at 65 °C for at least 4 hours. The inlet and outlet ports were punched through the peeled-off microchannel using a biopsy punching tool (Harris Uni-core). The PDMS microchannel was bonded to the glass microscope slide after exposing both in an oxygen plasma. The fabricated microchannels height were 10 µm, 18 µm, 25 µm, and 35 µm. A hydrofluoroether (HFE7500, 3M) containing 2% (v/v) fluorosilane (1H,1H,2H,2H-perfluorooctyl) was filled in the PDMS microchannel prior to drop generation. It increased the oil wetting by rendering the surface hydrophobic.

Electrode fabrication

On-chip electrodes were manufactured by injecting the melted indium (low melting point solder) into the custom-made microchannels for the electrodes.[31] The fabricated microfluidic device was placed on the hot plate at 95 °C during the infusion of low melting point solder while being fluidic. After connecting the electrodes with a metal connector (RND 205-00168, male header, Elfa Distrelec), the device was removed from the hotplate to solidify the metal electrodes.[32]

Alginate solution and Calcium chloride solution preparation

The alginate solution was prepared by dissolving powdered sodium alginate (PRONOVA UP LVM), or Fluoresceinamine labeled alginate (L. Hyperborea stipe) with FG = 0.68 and a M_W of 274 kDa (PROTANAL LF 2005) in deionized water that contains 300 mM mannitol (TCI). Calcium chloride ($CaCl_2$) solution was prepared by dissolving $CaCl_2.2H_20$ salt (MERCK) in deionized water that contains 150 mM mannitol, and subsequently, the pH of the solution was adjusted to 7.2 using sodium hydroxide. Mannitol was included in the formulations to reduce changes in local osmolarity associated with the ionotropic gelation and thus reduce concomitant adverse effects on the gel bead geometry.[17,33] Both the solutions were filtered through a 0.2 µm filter to remove undissolved residue before use.

Experimental setup

A microfluidic chip for droplet generation and subsequently picoinjection was mounted on an inverted microscope (Olympus IX 70) stage for visualization using an appropriate lens (4x, 10x, 20x, or 40x magnification). Pico-Surf™ 1 (2% (w/w) in Novec™ 7500) was used as a continuous phase. Three syringe pumps (NEMESYS, Cetoni GmbH, Germany) were used to control the volumetric flow by actuating the syringes connected to the microchannels with micro tubing (PE/2, Scientific Commodities). The potential set up by the on-chip electrodes was controlled connecting at a high voltage amplifier (623B, TREK) through copper wires (metal connector, 175448, female header, Elfa Distrelec). A waveform generator (33600A, Keysight) was used to generate a signal at 25 kHz frequency and amplitude 100 mV that was amplified up to 1.7 V_{pp} by the high voltage amplifier before feeding to the on-chip electrodes. A high-speed camera (FASTCAM SA3, Photron, model: 120K M1) was used to capture the images. The collected alginate beads were transformed into the aqueous medium (10 mM $CaCl_2$) using emulsion breaking solution (Pico-Break 1, Sphere Fluidics). The microgel particles were analyzed using a 63X water lens of a confocal laser scanning microscope (LEICA TCS SP8). Some of the samples were analyzed using different lenses (10X, 40X water) of quantitative phase-contrast imaging (Phi Optics, spatial light interference microscopy, LEICA Z1). The ImageJ (http://imagej.nih.gov/ij/) image processing software was used to process captured microscopic images.

Microgel beads fabrication

The employed microfluidic setup for monodisperse microgel bead fabrication consists of a droplet generation and a picoinjection module downstream from the droplet generation site integrated with the same microfluidic chip (Fig. 1). The PDMS device contains microfluidic feed channels for the liquids

needed for the initial emulsification and a supply channel for the picoinjected volume serving as the gelation platform. A separate set of channels is designed adjacent to the fluidic picoinjection channel in the PDMS device and filled with electrically conducting material to generate the electric field in the proximity of the picoinjection site. The electrical field induces a merger of the picoinjected volume in the droplet in the main chain channel in an electrocoalescence process.[34,35]

In the first approach, chelate free aqueous Ca^{2+} is injected into an aqueous emulsion droplet containing Na-alginate in the solution state (Fig. 1(a)). The device is first emulsifying the aqueous alginate pre-gel solution to homogeneously sized droplets dispersed in the oil phase using flow-focusing. The aqueous alginate droplets are subsequently squeezed into the picoinjector downstream from the first collection domain. In the picoinjector, aqueous Ca^{2+} solution is injected into each emulsion droplet, thus inducing the sol-gel transition, and further transported to the device's final collection region. Following breakage (destabilization) of the emulsion, the aqueous microgel beads are collected. In this approach, the resulting microgel population's size is controlled by the emulsion size droplet generated in the flow focusing part of the device and can be tuned by user-selected dimensions of the microfluidic channels and operating process parameters.

In the second approach, Na-alginate in the solution state is injected into an aqueous emulsion droplet of chelate free aqueous Ca^{2+} (Fig. 1(b)); an inverse strategy as compared to the first approach. The device is first emulsifying the aqueous Ca^{2+} solution to homogeneously sized droplets dispersed in the oil phase using the flow-focusing approach. These aqueous droplets are subsequently squeezed into the picoinjector downstream from the flow focusing region. In the picoinjector, aqueous alginate pre-gel solution is injected into each emulsified Ca-containing droplet and further transported to the final collection part of the device.

Following the destabilization of the emulsion, the alginate gel beads are collected. In this approach, the size of the resulting microgel population is mainly controlled by the picoinjected volume of the alginate solution and can be controlled by the user-selected dimensions of the injection channel and injector (average flow rate).

Results and discussion

Production of Ca-alginate beads by the picoinjection of $CaCl_2$ solution inside aqueous Na-alginate emulsified droplets

The homogeneously sized Ca-alginate beads were prepared by following a single-step microgel synthesis process (Fig. 2(a)). An evenly spaced aqueous Na-alginate droplets, produced by a flow-focusing method at ~1.1 kHz rate, were picoinjected with 100mM aqueous $CaCl_2$ assisted by the actuation of an electric field due to electrocoalescence. The flow rates of the Na-alginate solution and the oil phase were 50 µl/hr and 500 µl/hr. The picoinjection flowrate of 5 µl/hr resulted in a concentration of 15mM $CaCl_2$ in the picoinjected droplet. The picoinjection of the aqueous Ca^{2+} initiated the gelation of the alginate pre-gel solution, and the duration of picoinjection of about in the order of 0.6 ms (Fig. 2(b)) is significantly shorter than the 400 – 800 ms reported to complete the formation of Ca mediated guluronic acid extended junction zone.[36] The rate of transformation of the alginate from the sol to the gel state being significantly slower than the rate for completion of the coalescence of the picoinjected volume in the emulsified droplet appears to be an essential factor reducing possible clogging effects in the process. The evenly spaced alginate droplets ensured an equal amount of Ca^{2+} being picoinjected in each droplet and combined with the short injection time as compared to time constants for the junction zone formation, yielded size uniformity of the microgels and lack of heterogeneity of the structure. The CLSM phase-contrast images of the microgels captured after transfer into an aqueous medium (10 mM $CaCl_2$) reveal the resultant microgel beads' high monodispersity (Fig. 2(c)). The alginate beads' internal morphology was illustrated using fluorescently labeled alginate and visualizing the beads using the confocal fluorescence microscopy (Fig. 2(d)). Mannitol was included in the aqueous phases in the processes to reduce possible adverse effects associated with local changes in osmolarity in the gelation process, thus setting up concentration/activity gradients similar to that driving formation of alginate concentration differences in the alginate gels prepared by diffusion.[37] Employing the present picoinjection strategy and solution compositions without mannitol yields more heterogeneous microgel beads

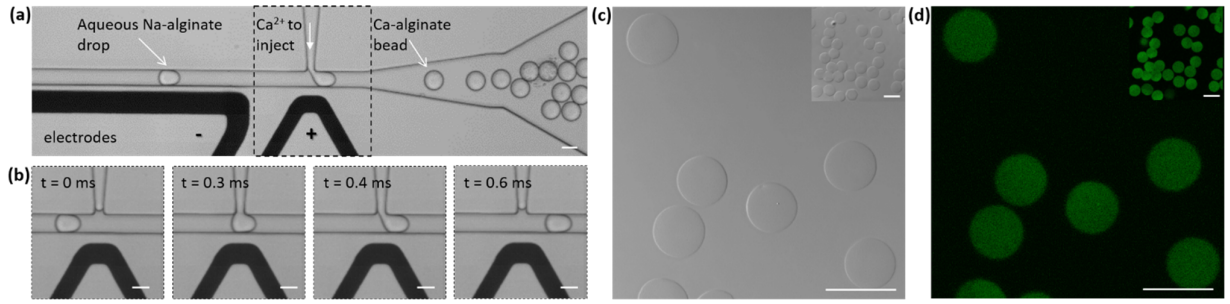

Fig. 2 One-step synthesis of monodisperse spherical alginate gel beads. (a) Optical micrograph of the microfluidic picoinjection device used to produce monodisperse Ca-alginate beads. (b) Experimental images of the time-sequence of the injection step. The gelation was initiated as the Na-alginate drop was injected with the Ca^{2+} ion from the perpendicular picoinjection channel upon the electrodes' activation of an electric field. The injection stage was completed at 0.6 ms. (c, d) Confocal microscope phase-contrast and fluorescent images of the Ca-alginate microparticles immersed in an aqueous 10 mM $CaCl_2$ solution after breaking the emulsion. These micrographs indicate the homogenous size and structurally homogenous alginate beads, respectively. Scale bars, 25 µm.

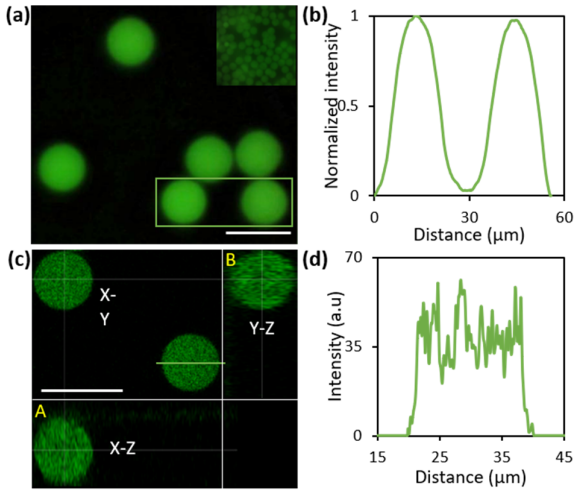

Fig. 3(a) Fluorescent images of the homogenously structured Ca-alginate bead inside an aqueous medium. Scale bar, 25 μm. (b) The fluorescence intensity profile across the two alginate beads (highlighted with a green rectangle in (a)) shows even intensity inside each microbead. (c) The CLSM fluorescent image stack of alginate microbead, orthogonal sectioning reveals the particle sphericity. A is Z-projection in the X–Z direction, and B is Z-projection in the Y–Z direction. Scale bar, 25 μm (pixel size X, Y, Z: 0.21, 0.21, 1 μm). (d) The intensity profile at the equatorial microbead cross-section shows the spatial distribution of alginate in the microbead.

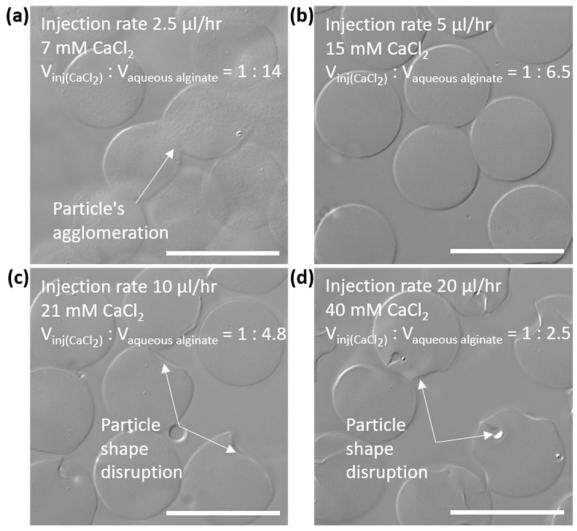

Fig. 4 Optimization of gelation parameters. Microscopic images of Ca-alginate microgel beads formed with different injection rates ((a) 2.5 μl/hr, (b) 5 μl/hr, (c) 10 μl/hr, (d) 20 μl/hr) of Ca^{2+} (100 mM initial concentration) inside aqueous alginate emulsion results in different concentrations of $CaCl_2$ inside the final droplet. The height and width of the microchannel were 18 and 25 μm, respectively. Scale bar, 25 μm.

(Fig. S2) illustrates the effect of local changes in the osmolarity associated with ionotropic gelation on the overall gel bead formation. Inclusion of mannitol in processes for alginate-based live-cell encapsulation is used and not stated to induce effects on cell viability.[38]

The fluorescence intensity is consistent all over the particles indicate that the alginate concentration is homogeneous throughout the microbeads. The fluorescent micrographs show a similar intensity level and distribution in each bead (Fig. 3(a)), which is verified by the intensity profile across the two particles presented in Fig. 3(b). Moreover, the particle was optically sliced to generate a stack of images in the Z-direction. The orthogonal projections of the slices in Z-series (X-Z and Y-Z) (Fig. 3(c)) further validate the spherical shape of the particles. Furthermore, the fluorescence intensity profile across the particle's cross-section indicates an average level throughout the bead, not systematically depending on the position (Fig. 3(d)). The fluctuations around the mean also evident in such data could originate from local alginate chain and fluorescence labeling concentration differences, e.g., due to heterogeneous pore size distribution. Overall, the data is interpreted as expected for a homogeneous alginate microbead without the systematic distributions reported for 0.5 mm Ca-alginate gel beads under some conditions.[33]

Characterization of gelation conditions: The height of the microfluidic channel and flow conditions were optimized for the fabrication of spherical and stable microgel beads. The flow rate of the dispersed (1% alginate, Q_D = 50 μl//hr) and continuous phase (oil, Q_C = 500 μl//hr) for drop generation were kept constant, while the flow rate of the picoinjection was varied between 2.5 and 20 μl//hr to assess the effect on the obtained alginate microbeads. Initially, the same concentration of 100 mM of $CaCl_2$ was used for the picoinjection, which resulted in Ca^{2+} concentration inside the droplet depending on the injection rate. Employing an injection rate of 2.5 μl//hr resulted in 7mM $CaCl_2$ inside the aqueous alginate droplet, which was found not to yield a stable microgel bead. In this case, most of the beads agglomerated after the emulsion destabilization and isolation from the carrier oil and transferred to the aqueous 10 mM $CaCl_2$ (Fig. 4(a)). Increasing the flow rate to 5 μl//hr yielded alginate microgel beads that were found not to agglomerate following replacing the oil phase with the aqueous phase (Fig. 4(b)).

Further increase in the injection rate to 10 μl//hr and 20 μl//hr resulted in 21 mM and 40mM $CaCl_2$ inside the final drop, which was ample for gelation. However, this resulted in non-spherical microgel beads due to the fast ionic crosslinking of alginate beads proceeding while in the confined channel (Fig. 4(c,d)). Therefore, we chose a Ca^{2+} concentration of 15mM inside the alginate droplets and injected it to a volume of 15% of the resultant droplet volume.

Effect of flow rate and channel dimensions on particle size: Having established working conditions for the alginate and Ca^{2+} as the crosslinking ion, further optimizing the conditions and establishing strategies to control the mean size of the microbeads were conducted by varying the flow rate ratio (Q_D/Q_C) and microchannel aspect ratio. The oil flow rate (Q_C) was fixed to 500 μl/hr, while the flow rate of the alginate solution (Q_D) was varied between 12.5 and 100 μl/hr to produce monodisperse microgel samples with different average size.

The picoinjection (Q_P) flow rate was adjusted accordingly between 1-7.5 μl/hr to inject the optimized percentage (15%) of aqueous $CaCl_2$ inside the aqueous emulsion of alginate.

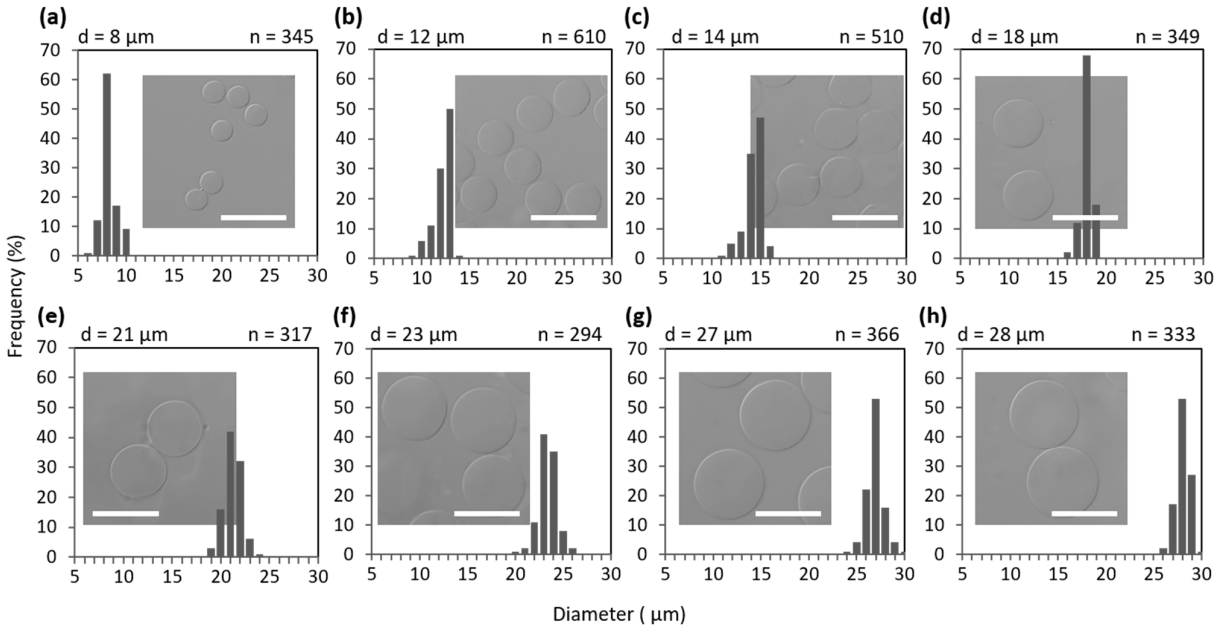

Fig. 5 The confocal microscope phase-contrast images of the prepared Ca-alginate microgels and corresponding size distribution histograms with 8, 12, 14, 18, 21, 27, and 28 µm mean diameter. The microgels were produced using five different cross-sectional dimensions (w×h) of the microfluidic channel ((a) 12.5×10, (b) 12.5×18, (c,d) 25×18, (e) 25×25, and (f-h) 25×35 $(\mu m)^2$). The employed flow conditions are summarized alongside the information of the obtained sizes in Table 1. Scale bars, 25 µm.

The size (S) of the bead was calculated by using the following relation

$$S = 2\sqrt{\frac{A}{\pi}}$$

where A is the projected area of the microgel. This parameter is the diameter of the spherical microgel, and thus the equivalent diameter for microgels deviating from a spherical shape.

Using Q_D equal to 12.5 µl/hr, yielded Ca-alginate beads with an average diameter of 8 µm and with a standard deviation (SD) of 0.76 µm (Fig. 5(a)). The picoinjection flow rate was 1 µl/hr, and a microfluidic device fabricated with a width and height of the microchannel of 12.5 and 10 µm, respectively, was employed. Increasing Q_D to 25 µl/hr and swapping to a device with a channel height of 18 µm increased the droplet volume, and consequently, the picoinjection flow rate was increased to 2 µl/hr to maintain the optimum Ca^{2+} concentration. The microgels fabricated under these conditions were found to have a diameter of 12 µm with a SD of 0.93 µm (Fig. 5(b)). Increasing the microchannel width further to 25 µm resulted in microbeads with a diameter of 14±0.87 µm (Fig. 5(c)). Using the same device and increasing Q_D to 50 µl/hr resulted in an increase in the alginate bead size to 18±0.52 µm (Fig. 5(d)). The picoinjection flow rates used in the two latter conditions were 2 and 5 µl/hr, respectively. The microchannel aspect ratio (w×h) of 25×25 $(\mu m)^2$ resulted in microbeads with an average diameter of 21±0.9 µm when the flow rate Q_D of 50 µl/hr was used and an injection flow rate of 4 µl/hr (Fig. 5(e)).

Further examples of obtained microbead sizes were obtained employing fixed microchannel dimensions (w=25µm, h= 35µm) and monitoring the microbead diameter prepared when Q_D was changed between 25 and 100 µl/hr. Q_D of 25, 50, and 100 µl/hr gives an average diameter 23±1.02, 27±0.88, and 28±0.65 µm, respectively (Fig. 5(f-h)). In these experiments, picoinjection flow rates of 2.5, 5, and 7.5 µl/hr were used to obtain the desired $CaCl_2$ concentration inside the aqueous alginate emulsion.

Furthermore, the increase in the Q_D by keeping the Q_C constant and thus increasing the flow rate ratio results in an increase in the average size of the microgel beads. The relationship between Q_D/Q_C, microchannel dimensions, and resulting microgel diameters are summarized in Table 1.

Table 1 Ca-alginate microbead size synthesized by picoinjection of aqueous Ca in emulsified droplets of aqueous alginate. The microbead size depended on microchannel dimensions (channel height and width at the drop junction and picoinjection) and flow rates ratio of the dispersed (Q_D) and continuous (Q_C) phase

Microchannel height (µm)	10	18		25	35
Microchannel width (µm)	12.5	12.5	25	25	25
Q_D/Q_C	Diameter of alginate bead ± SD (µm)				
0.025	8±0.76 (n=345)				
0.05		12±0.93 (n=610)	14±0.87 (n=510)		23±1.02 (n=294)
0.1			18±0.52 (n=349)	21±0.9 (n=317)	27±0.88 (n=366)
0.2					28±0.65(n=333)

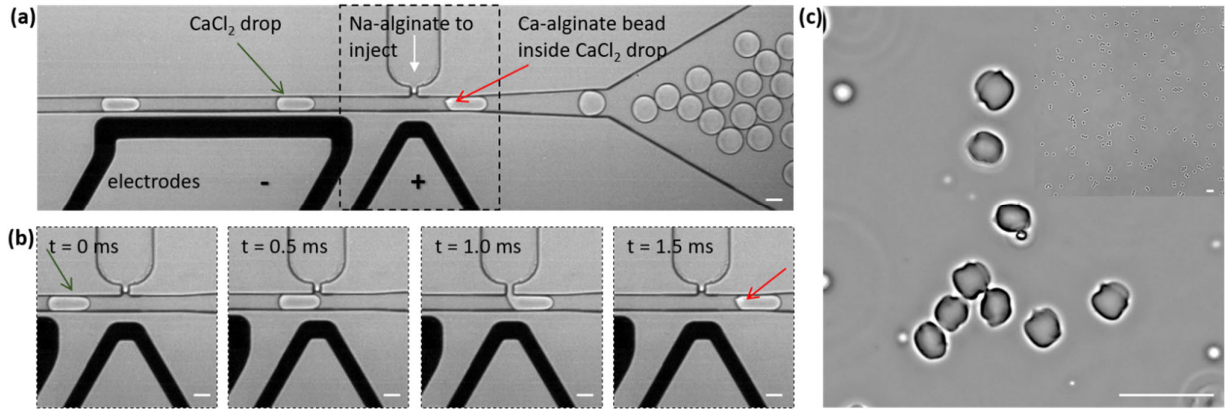

Fig. 6 Single-step synthesis of monodisperse non-spherical alginate gel beads. (a) Photographic image of the microfluidic picoinjection device used to fabricate monodisperse Ca-alginate beads. (b) Experimental images of the time-sequence of the injection step. The gelation was initiated by injection aqueous Na-alginate from the picoinjection channel into a drop containing Ca^{2+} where electrocoalescence of the adjacent droplets occurred in the electrical field set up using the adjacent electrodes. The injection phase was finished at 1.5ms. (c) Microscopic images of the resultant microgels inside an aqueous medium after emulsion break. The images reflect the shape of the microgel is non-spherical. Scale bars, 25 µm.

These data show that small-sized chelate-free Ca-alginate beads with diameters ranging from 8 to 28 µm with low SD (≤1 µm) were fabricated where the average size is controlled by selecting aspect ratios of the microchannel and varying Q_D/Q_C between 0.025 and 0.2. The low value of SD reveals that the obtained microgels samples can be considered essentially monodisperse.

Production of Ca-alginate beads by the picoinjection of Na-alginate solution in aqueous $CaCl_2$ emulsion droplets

This strategy to fabricate Ca-alginate beads is essentially the inverse of the first process (Fig. 1(b)). An aqueous 50mM $CaCl_2$ solution was first emulsified, followed by the picoinjection of 1% aqueous Na-alginate solution. A typical experimental picoinjection process is shown in Fig. 6(a). The aqueous emulsion of $CaCl_2$ drop before and after picoinjection of Na-alginate solution is highlighted with a green and red arrow, respectively. The flow rates of the dispersed phase (aqueous $CaCl_2$) and the oil phase were 100 µl/hr (Q_D) and 500 µl/hr (Q_C), respectively. The flow rate (Q_P) of the injection channel was 5 µl/hr. The picoinjection process of the alginate solution into the $CaCl_2$ drop was completed in 1.5ms (Fig. 6(b)).

The equal spacing between the initially emulsified droplets due to the consistent drop generation flow rates ensured an equal volume being picoinjected for increased monodispersity of the microgel beads. The optical micrographs of the microgel beads after breaking the emulsion and removing the oil (Fig. 6(c)) indicate that this process yielded non-spherical beads.

Effect of $CaCl_2$ concentration on the size and shape of the microgels: The influence of the concentration of $CaCl_2$ on the size and shape of the microgels were investigated by using constant Q_C, Q_D, and Q_P equal to 100, 500, and 10 µl/hr, respectively, while the concentration of the solution containing Ca^{2+} was varied from 10 to 100 mM. Fig. 7(a) shows micrographs of the obtained particles prepared using various concentrations of the $CaCl_2$ solution. An averaged feret diameter (longest distance between two points) was used to characterize the size of the bead (Fig. 7(b)), and the averaged values of circularity were used as a parameter for the shape of the microgels.

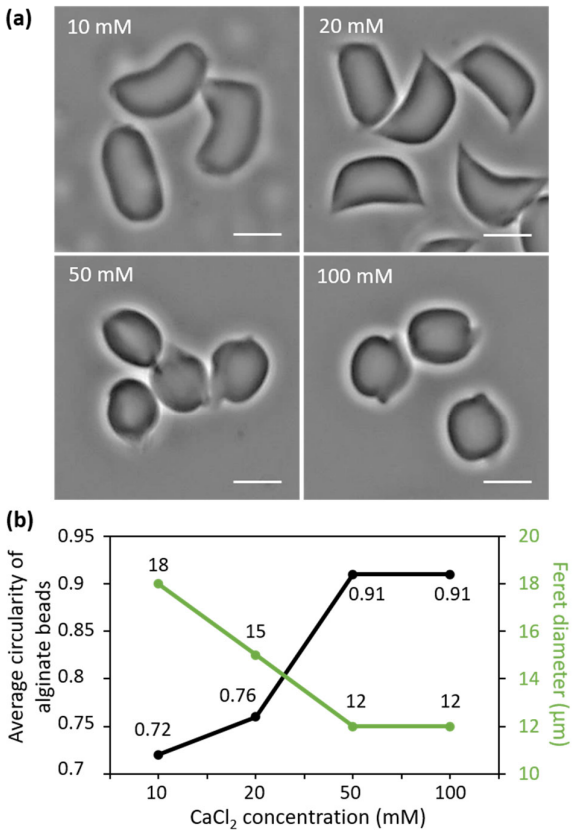

Fig. 7 Optical micrographs using SLIM quantitative phase-contrast of alginate microbeads produced by the injection of alginate solution in various concentrations of $CaCl_2$ aqueous droplets. Scale bars are 10 µm. (b) The average circularity of the microbeads and their feret diameters versus $CaCl_2$ concentration in the aqueous droplet.

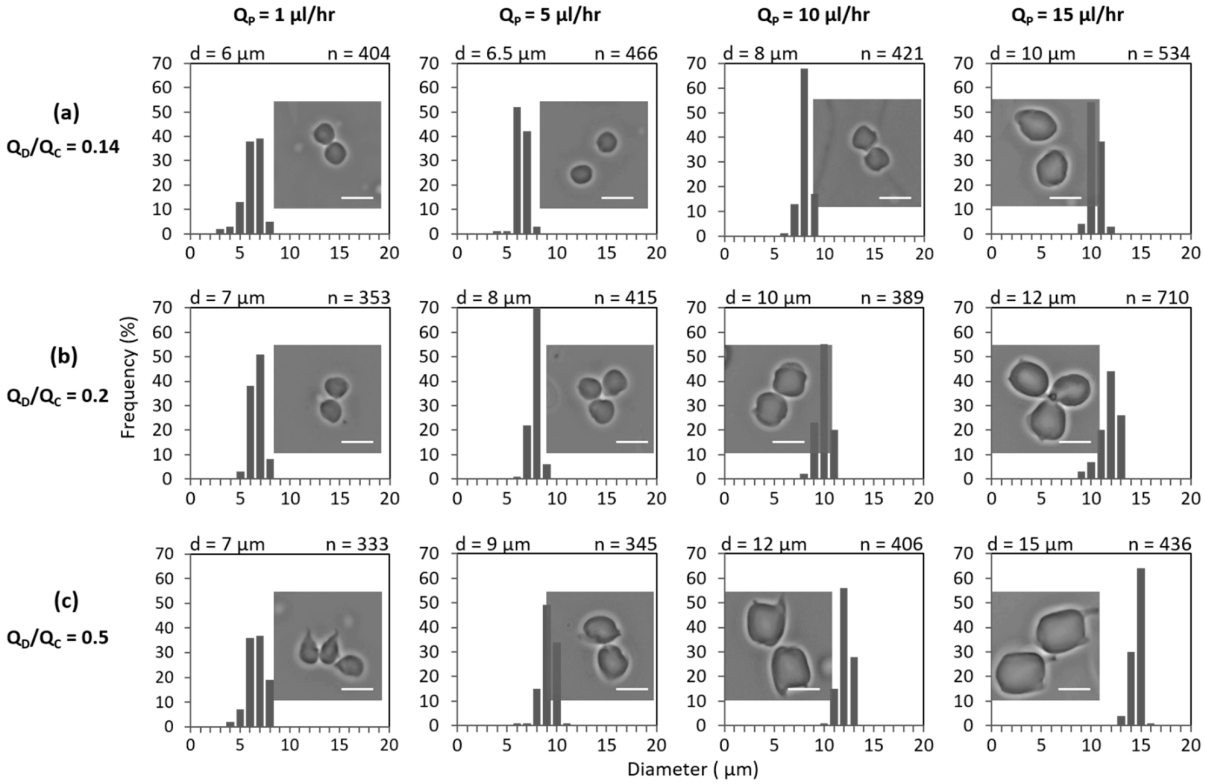

Fig. 8 The SLIM quantitative phase-contrast images of the resultant microgels and their size distribution at (a) Q_D/Q_C = 0.14, (b) Q_D/Q_C = 0.2 and (c) Q_D/Q_C = 0.5. The cross-section of the microfluidic device was 25×35 (µm)^2. The flow rate of the dispersed phase was 100 µl/hr. The oil phase flow rate was varied in the range between 200-700 µl/hr to produce different sized gels. The picoinjection flow rate was varied between 1 and 15µl/hr. The images reflect the microgels are non-spherical. Scale bars, 10 µm.

The circularity defined as

$$C = \frac{4\pi A}{P^2}$$

where A and P are the projected area and perimeter of the microbead, respectively, were estimated based on the obtained micrographs for individual microbeads and averaged for a large number of beads.

Effect of flow rates on the size and circularity of the microgels: The sizes of the alginate microbeads prepared by injecting aqueous alginate in Ca-containing droplets were determined at various flow rates Q_C and Q_P. The Q_D was 100 µl/hr, and the flow rates of oil 700, 500, and 200 µl/hr, results in the flow rate ratios (Q_D/Q_C) of 0.14, 0.2, and 0.5, respectively. The picoinjection flow rate Q_P was varied between 1 and 15 µl/hr for each of the dispersed / continuous flow rate ratios.

Microgel beads with an average size of 6 µm and with a SD of 0.96 µm were obtained for at picoinjection flow rate of Q_P was 1 µl/hr when Q_D/Q_C was 0.14 (Fig. 8(a)). Increasing Q_P to 5 µl/hr did not significantly change the average size (6.5 µm) of the microbeads, but a decrease in the width of the size distribution (to SD equals 0.55 µm) possibly due to improved matching of injection rate relative to the rate of drop generation, was observed. Further increase of the picoinjection rate Q_P to 10 and 15 µl/hr, yielded larger microbeads, e.g., the average size ± SD increased to 8±0.54 and 10±0.56 µm, respectively. A similar trend in the impact of the picoinjection flow rate on the resulting microbead size was observed at Q_D/Q_C equal to 0.2 (Fig. 8(b)). For Q_P of 1, 5, 10, and 15 µl/hr, the microbead sizes were found to be 7±0.57, 8±0.49, 10±0.63, and 12±0.95 µm, respectively. Further increase in Q_D/Q_C to 0.5 increased the size of the microgel bead against each studied injection flow rate (Fig. 8(c)). The mean size ± SD were 7±0.86, 9±0.71, 12±0.63, and 15±0.55 µm when Q_P was 1, 5, 10, and 15 µl/hr. The microgel beads' produced sizes using different flow rates of the oil, $CaCl_2$, and Na-alginate solutions are summarized in Table 2. Overall, this data documents that the sizes and shapes of the generated microbeads were controlled by the drop generation and picoinjection flow rates. The trends in the effect of Q_D/Q_C and Q_P on the final size and circularity of the microgel bead are in Fig. 9(a) and Fig. 9(b).

As the picoinjection flow rate increased, the volume of aqueous alginate increased inside the $CaCl_2$ drop. The concomitant increase in the alginate bead's size indicates the injected volume is the main parameter in controlling the size. Alternatively, in other words, diffusion of alginate inside the $CaCl_2$ droplet following picoinjection is not largely affecting the size before the sol-gel transition practically prohibits further microgel bead increase in size. However, the circularity decreased due to the further pulling of alginate solution along the confined channel by $CaCl_2$ drop.

Table 2 Size of Ca-alginate microgels prepared by picoinjection aqueous alginate in emulsified aqueous Ca^{2+} depending on the flow rates ratio of the drop generation (dispersed (Q_D) and continuous (Q_C) phase), and picoinjection flowrate (Q_P). Overall, an increase in the Q_D/Q_C and Q_P results in an increased size of the alginate microgel. The width and height of the microchannel were 25 and 35 µm, respectively

Q_P (µl/hr)	1	5	10	15
Q_D/Q_C	Diameter of alginate microgel ± SD (µm)			
0.14	6±0.96 (n=404)	6.5±0.55 (n=466)	8±0.54 (n=421)	10±0.56 (n=534)
0.2	7±0.57 (n=353)	8±0.49 (n=415)	10±0.63 (n=389)	12±0.95 (n=710)
0.5	7±0.86 (n=333)	9±0.71 (n=345)	12±0.63 (n=406)	15±0.55 (n=436)

When we set the Q_D/Q_C to 0.14 and increased the Q_P from 1 to 15 µl/hr, the microgel's size increased from 6 to 10 µm, while the circularity decreased from 0.94 to 0.90. Correspondingly, when Q_D/Q_C was increased to 0.2 and Q_P was changed similarly, the gel beads' size increased from 7 to 12 µm, whereas the circularity decreased from 0.94 to 0.89. The alginate bead's size increased from 7 to 15 µm when the Q_D/Q_C was set to 0.5, and Q_P varied from 1 to 15 µl/hr. The circularity was decreased from 0.92 to 0.86.

For a fixed value of Q_P, the size of the gel beads increased as we increased the Q_D/Q_C because the volume of $CaCl_2$ drop and, consequently, the contact area with the injection channel increased. Therefore, the circularity of the resultant bead decreased due to the confined channel and fast ionic crosslinking. In other words, as we increased the volume of the $CaCl_2$ emulsion, the length of the squeezed droplets in the picoinjector downstream increased. Subsequently, more solution from the picoinjector was injected into the droplet results in a large size and low circularity of the final bead.

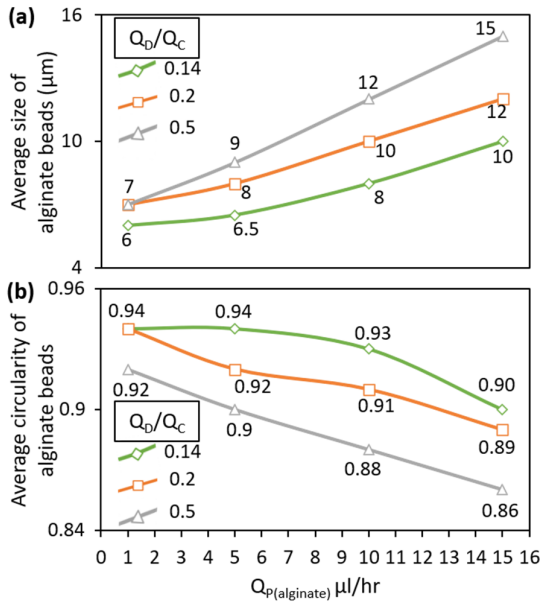

Fig. 9 (a) Size of the alginate bead's dependence on dispersed, continuous, and picoinjection flow rate. The microgel's size increases as the value of Q_D/Q_C increased or more significantly with the increase of injection flowrate of aqueous Na-alginate. (b) The dependence of resultant microgel circularity on dispersed, continuous, and picoinjection flow rate. The microbeads' average circularity decreased with the increase in Q_D/Q_C and the picoinjection flow rate.

This data clearly indicates that the selection of the flow rates (Q_D, Q_C, Q_P) effectively controls the size and, to some extent, the shape of the resulting microgels formed for a given set of channel dimensions.

Conclusions

We reported a novel picoinjection-based microfluidic platform for the production of chelate free Ca-alginate beads by the picoinjection of aqueous $CaCl_2$ into the emulsion of Na-alginate solution and vice versa. The duration of the droplet merger in the electrocoalescence of the picoinjection site in the order of 0.2-0.4 ms being much less than the typical time for the Ca-mediated junction formation in the gelation process, is reducing the risk of clogging the device and contributes to ensuring operation of extended time periods. By user selection of the dimensions in the microfluidic channels of the device at the stage of fabrication, and control of the concentrations and flow rates, it is shown that alginate microbeads in size range from 8 to 28 µm diameter were readily prepared by picoinjection ionic crosslinker into the emulsified aqueous droplets of alginate in its pre-gel state. This is a range which at least the upper range can be extended. In this process, the size of the resulting microgel is controlled by the size of the aqueous alginate droplet, possibly due to the distribution of the Ca as a crosslinker following picoinjection throughout the volume of the alginate droplet. Picoinjection of aqueous alginate in emulsified aqueous Ca appears to yield microgel sizes controlled by the picoinjection volume, e.g., the aqueous phase with the least diffusive component involved directly in the ionotropic sol-gel transition. Also, in this strategy, user control of flow parameters offers direct control of the resulting microgels sizes, with examples of mean sizes in the range from 6 to 15 µm in equivalent diameter being explicitly demonstrated. A further facet is that the latter picoinjection strategy additionally offers an option also to prepare non-spherical microgels. As the diffusion of the alginate prior to the sol-gel transition appears not to be largely affecting the size of the microgels in this strategy, a reduction of the chain length could offer an additional means to control the microgels' size.

The success of the picoinjection strategy showing that one can form alginate microgels in a clog-free operation appears to be related to the duration of the picoinjection process relative to the characteristic duration of the sol-gel transition, thus indicating that also other systems can be of interest to explore in such a context. Examples of systems include, e.g., pectin,

gellan gum, and carrageenan to be crosslinked with gel inducing ions. In these cases, it appears feasible to explore the picoinjection route to provide chelate free microgels, as suitable to explore for various applications.

Authors' contributions

H.A. and B.T.S. conceived the research. B.T.S. supervised the research. H.A designed the experiments. H.A. performed the experiments. H.A and B.T.S. contributed to the manuscript preparation. All authors have given approval to the final version of the manuscript.

Conflict of interest

There are no conflicts to declare.

Acknowledgements

This work is supported by the Research Council of Norway, Norwegian Micro- and Nano-Fabrication Facility, NorFab, project number 245963/F50. The authors gratefully acknowledge the gift of the fluorescently labeled alginate from Dr. Berit L Strand, Dept of Food Science and Biotechnology, NTNU, Trondheim.

References

(1) Lee, K. Y.; Mooney, D. J. Alginate: Properties and Biomedical Applications. *Prog. Polym. Sci.* **2012**, *37* (1), 106–126.

(2) Morimoto, Y.; Onuki, M.; Takeuchi, S. Mass Production of Cell-Laden Calcium Alginate Particles with Centrifugal Force. *Adv. Healthc. Mater.* **2017**, *6* (13), 1–5.

(3) Ching, S. H.; Bansal, N.; Bhandari, B. Alginate Gel Particles–A Review of Production Techniques and Physical Properties. *Crit. Rev. Food Sci. Nutr.* **2017**, *57* (6), 1133–1152.

(4) Morris, E. R.; Nishinari, K.; Rinaudo, M. Gelation of Gellan - A Review. *Food Hydrocoll.* **2012**, *28* (2), 373–411.

(5) Sun, J.; Tan, H. Alginate-Based Biomaterials for Regenerative Medicine Applications. *Materials (Basel).* **2013**, *6* (4), 1285–1309.

(6) Gombotz, W. R.; Wee, S. F. Protein Release from Alginate Matrices. *Adv. Drug Deliv. Rev.* **1998**, *31* (3), 267–285.

(7) Martinez, C. J.; Kim, J. W.; Ye, C.; Ortiz, I.; Rowat, A. C.; Marquez, M.; Weitz, D. A Microfluidic Approach to Encapsulate Living Cells in Uniform Alginate Hydrogel Microparticles. *Macromol. Biosci.* **2012**, *12* (7), 946–951.

(8) Lanza, R. P.; Hayes, J. L.; Chick, W. L. Encapsulated Cell Technology. *Nat. Biotechnol.* **1996**, *14* (9), 1107–1111.

(9) Yao, L. S.; Liu, T. Q.; Ge, D.; Cui, Z. F.; Ma, X. H. Culture of Neural Stem Cells in Alginate Microbeads. *Chinese J. Biomed. Eng.* **2007**, *26* (1), 126–133.

(10) Swioklo, S.; Ding, P.; Pacek, A. W.; Connon, C. J. Process Parameters for the High-Scale Production of Alginate-Encapsulated Stem Cells for Storage and Distribution throughout the Cell Therapy Supply Chain. *Process Biochem.* **2017**, *59*, 289–296.

(11) Andersen, T.; Auk-Emblem, P.; Dornish, M. 3D Cell Culture in Alginate Hydrogels. *Microarrays* **2015**, *4* (2), 133–161.

(12) Read, G. H.; Miura, N.; Carter, J. L.; Kines, K. T.; Yamamoto, K.; Devasahayam, N.; Cheng, J. Y.; Camphausen, K. A.; Krishna, M. C.; Kesarwala, A. H. Three-Dimensional Alginate Hydrogels for Radiobiological and Metabolic Studies of Cancer Cells. *Colloids Surfaces B Biointerfaces* **2018**, *171* (August 2017), 197–204.

(13) Shintaku, H.; Kuwabara, T.; Kawano, S.; Suzuki, T.; Kanno, I.; Kotera, H. Micro Cell Encapsulation and Its Hydrogel-Beads Production Using Microfluidic Device. *Microsyst. Technol.* **2007**, *13* (8–10), 951–958.

(14) Zhang, L.; Chen, K.; Zhang, H.; Pang, B.; Choi, C. H.; Mao, A. S.; Liao, H.; Utech, S.; Mooney, D. J.; Wang, H.; et al. Microfluidic Templated Multicompartment Microgels for 3D Encapsulation and Pairing of Single Cells. *Small* **2018**, *14* (9), 1–8.

(15) Kamaruddin, M. A.; Yuso, M. S.; Aziz, H. A. Preparation and Characterization of Alginate Beads by Drop Weight. *Int. J. Technol.* **2014**, *5* (2), 121–132.

(16) Zhang, Z. H.; Sun, Y. S.; Pang, H.; Munyendo, W. L. L.; Lv, H. X.; Zhu, S. L. Preparation and Evaluation of Berberine Alginate Beads for Stomach-Specific Delivery. *Molecules* **2011**, *16* (12), 10347–10356.

(17) Strand, B. L.; Gåserød, O.; Kulseng, B.; Espevik, T.; Skjåk-Bræk, G. Alginate-Polylysine-Alginate Microcapsules: Effect of Size Reduction on Capsule Properties. *J. Microencapsul.* **2002**, *19* (5), 615–630.

(18) Olesen, M. T. J.; Winther, A. K.; Fejerskov, B.; Dagnaes-Hansen, F.; Simonsen, U.; Zelikin, A. N. Bi-Enzymatic Embolization Beads for Two-Armed Enzyme-Prodrug Therapy. *Adv. Ther.* **2018**, *1* (4), 1800023.

(19) Xie, J.; Wang, C. H. Electrospray in the Dripping Mode for Cell Microencapsulation. *J. Colloid Interface Sci.* **2007**, *312* (2), 247–255.

(20) Watanabe, H.; Matsuyama, T.; Yamamoto, H. Experimental Study on Electrostatic Atomization of Highly Viscous Liquids. *J. Electrostat.* **2003**, *57* (2), 183–197.

(21) Sugiura, S.; Oda, T.; Aoyagi, Y.; Matsuo, R.; Enomoto, T.; Matsumoto, K.; Nakamura, T.; Satake, M.; Ochiai, A.; Ohkohchi, N.; et al. Microfabricated Airflow Nozzle for Microencapsulation of Living Cells into 150 Micrometer Microcapsules. *Biomed. Microdevices* **2007**, *9* (1), 91–99.

(22) Sugiura, S.; Oda, T.; Izumida, Y.; Aoyagi, Y.; Satake, M.; Ochiai, A.; Ohkohchi, N.; Nakajima, M. Size Control of Calcium Alginate Beads Containing Living Cells Using Micro-Nozzle Array. *Biomaterials* **2005**, *26* (16), 3327–3331.

(23) Velasco, D.; Tumarkin, E.; Kumacheva, E. Microfluidic Encapsulation of Cells in Polymer Microgels. *Small* **2012**, *8* (11), 1633–1642.

(24) Zhang, H.; Tumarkin, E.; Sullan, R. M. A.; Walker, G. C.; Kumacheva, E. Exploring Microfluidic Routes to Microgels of Biological Polymers. *Macromol. Rapid Commun.* **2007**,

28 (5), 527–538.

(25) Utech, S.; Prodanovic, R.; Mao, A. S.; Ostafe, R.; Mooney, D. J.; Weitz, D. A. Microfluidic Generation of Monodisperse, Structurally Homogeneous Alginate Microgels for Cell Encapsulation and 3D Cell Culture. *Adv. Healthc. Mater.* **2015**, *4* (11), 1628–1633.

(26) Shao, F.; Yu, L.; Zhang, Y.; An, C.; Zhang, H.; Zhang, Y.; Xiong, Y.; Wang, H. Microfluidic Encapsulation of Single Cells by Alginate Microgels Using a Trigger-Gellified Strategy. *Front. Bioeng. Biotechnol.* **2020**, *8* (October), 1–13.

(27) Håti, A. G.; Bassett, D. C.; Ribe, J. M.; Sikorski, P.; Weitz, D. A.; Stokke, B. T. Versatile, Cell and Chip Friendly Method to Gel Alginate in Microfluidic Devices. *Lab Chip* **2016**, *16* (19), 3718–3727.

(28) Oliveira, A. F.; Bastos, R. G.; de la Torre, L. G. Bacillus Subtilis Immobilization in Alginate Microfluidic-Based Microparticles Aiming to Improve Lipase Productivity. *Biochem. Eng. J.* **2019**, *143* (August 2018), 110–120.

(29) Bardsley, W. G.; Childs, R. E.; Crabbe, M. J. C. Inhibition of Enzymes by Metal Ion Chelating Reagents. The Action of Copper Chelating Reagents on Diamine Oxidase. *Biochem. J.* **1974**, *137* (1), 61–66.

(30) Ahmed, H.; Destgeer, G.; Park, J.; Jung, J. H.; Sung, H. J. Vertical Hydrodynamic Focusing and Continuous Acoustofluidic Separation of Particles via Upward Migration. *Adv. Sci.* **2018**, *5* (2), 1700285.

(31) Siegel, A. C.; Shevkoplyas, S. S.; Weibel, D. B.; Bruzewicz, D. A.; Martinez, A. W.; Whitesides, G. M. Cofabrication of Electromagnets and Microfluidic Systems in Poly(Dimethylsiloxane). *Angew. Chemie - Int. Ed.* **2006**, *45* (41), 6877–6882.

(32) Sjostrom, S. L.; Bai, Y.; Huang, M.; Liu, Z.; Nielsen, J.; Joensson, H. N.; Andersson Svahn, H. High-Throughput Screening for Industrial Enzyme Production Hosts by Droplet Microfluidics. *Lab Chip* **2014**, *14* (4), 806–813.

(33) Strand, B. L.; Mørch, Y. A.; Espevik, T.; Skjåk-Braek, G. Visualization of Alginate-Poly-L-Lysine-Alginate Microcapsules by Confocal Laser Scanning Microscopy. *Biotechnol. Bioeng.* **2003**, *82* (4), 386–394.

(34) Sjostrom, S. L.; Joensson, H. N.; Svahn, H. A. Multiplex Analysis of Enzyme Kinetics and Inhibition by Droplet Microfluidics Using Picoinjectors. *Lab Chip* **2013**, *13* (9), 1754–1761.

(35) Ahn, K.; Agresti, J.; Chong, H.; Marquez, M.; Weitz, D. A. Electrocoalescence of Drops Synchronized by Size-Dependent Flow in Microfluidic Channels. *Appl. Phys. Lett.* **2006**, *88* (26).

(36) Bowman, K. A.; Aarstad, O. A.; Nakamura, M.; Stokke, B. T.; Skjåk-Bræk, G.; Round, A. N. Single Molecule Investigation of the Onset and Minimum Size of the Calcium-Mediated Junction Zone in Alginate. *Carbohydr. Polym.* **2016**, *148*, 52–60.

(37) Skjåk-Bræk, G.; Grasdalen, H.; Smidsrød, O. Inhomogeneous Polysaccharide Ionic Gels. *Carbohydr. Polym.* **1989**, *10* (1), 31–54.

(38) Bochenek, M. A.; Veiseh, O.; Vegas, A. J.; McGarrigle, J. J.; Qi, M.; Marchese, E.; Omami, M.; Doloff, J. C.; Mendoza-Elias, J.; Nourmohammadzadeh, M.; et al. Alginate Encapsulation as Long-Term Immune Protection of Allogeneic Pancreatic Islet Cells Transplanted into the Omental Bursa of Macaques. *Nat. Biomed. Eng.* **2018**, *2* (11), 810–821.

1